Synthesis of high quality p-type Zn_3P_2 nanowires and their application in MISFETs

C. Liu,[a] L. Dai,*[a] L. P. You,[ab] W. J. Xu,[a] R. M. Ma,[a] W. Q. Yang,[a] Y. F. Zhang[a] and G. G. Qin*[a]

Received 30th May 2008, Accepted 3rd July 2008
First published as an Advance Article on the web 16th July 2008
DOI: 10.1039/b809245a

Single-crystalline Zn_3P_2 nanowires (NWs) have been synthesized on silicon (Si) substrates *via* a vapor phase transport method. Zn (99.99%) powder and InP (99.99%) fragments were used as the sources, and 10 nm thick thermal evaporated gold (Au) film was used as the catalyst. The as-prepared Zn_3P_2 NWs have diameters of 100–200 nm and lengths of more than 10 μm. Single NW metal–insulator–semiconductor field-effect transistors (MISFETs) based on Zn_3P_2 NWs were fabricated. Electrical transport measurements show that the as-grown Zn_3P_2 NWs are of p-type. The hole concentrations and mobilities of the p-type Zn_3P_2 NWs are about 5.6×10^{16} cm^{-3} and 42.5 cm^2 V^{-1} s^{-1}, respectively. The on–off ratio of the MISFET is about 4×10^4, and its threshold voltage and transconductance are 2.5 V and 35 nS, respectively. These parameters indicate that the p-type Zn_3P_2 NWs are of high quality, and may have potential applications in nanoscale electronic and optoelectronic devices.

Introduction

Semiconductor nanowires (NWs) are good candidates for building blocks for functional nanodevices.[1–7] Using the bottom-up method, high performance field-effect transistors (FETs) have been fabricated with NWs on various substrates.[7–15] To date, n-channel metal–oxide–semiconductor (NMOS)[8,13,14] and n-channel metal–semiconductor (NMES)[15] logic gates have been fabricated with both single NWs and NW thin films. Complementary logic gates, *e.g.* the complementary metal–oxide–semiconductor (CMOS) NOT logic gate, involving both n- and p-channel transistors, have a key characteristic of low static power dissipation, which is especially superior in ever denser circuit integration. However, due to the lack of high quality p-type semiconductor NWs, the progress in the study of NW CMOS fabricated by the bottom-up method is quite slow.[7] Besides, the high quality p-type semiconductor NWs have potential applications in nano-optoelectronic devices such as light-emitting diodes and laser diodes.

Zn_3P_2 is a group II_3–V_2 semiconductor material with a direct band gap in the range of 1.5–1.6 eV, the optimum range for solar energy conversion. It has potential applications in optoelectronic devices, such as light-emitting diodes, electro-optic detectors, sensors, and solar cells.[16–19] To date, some work has been done on synthesis of Zn_3P_2 nanostructures.[16,20–24] However, to the best of our knowledge, so far only one work reported electronic devices based on Zn_3P_2 NWs.[16] In this communication, we report a chemical vapor deposition (CVD) method to synthesis p-type Zn_3P_2 NWs, and we also report the fabrication of Zn_3P_2 single NW (SNW) metal–insulator–semiconductor field-effect transistors (MISFETs) for the first time.

Experimental

Zn_3P_2 NWs were synthesized *via* the CVD method in a tube furnace. First, a mixture of Zn (99.99%) powder and InP (99.99%) fragments (in a ratio of 1 : 1 by mass) was placed on a quartz boat as the source. Then pieces of Si wafer covered with 10 nm thick thermally evaporated Au catalyst films, as the substrates, were loaded on the quartz boat 10–15 cm downstream from the source. The boat was then inserted into the center of a quartz tube inside the tube furnace. After being cleaned with Ar (99.999%) gas, the quartz tube was rapidly heated to 850 °C. The synthesis duration was 1 h with a constant Ar flow rate of 140 sccm at atmospheric pressure. After the synthesis process, yellowish products were found on the substrates and characterized using a field emission scanning electron microscope (FESEM) (Amray 1910 FE), a high-resolution transmission electron microscope (HRTEM) (Tecnai F30) equipped with an energy-dispersive X-ray (EDX) spectroscope and a high-angle angular dark-field scanning transmission electron microscope (HAADF-STEM). The photoluminescence (PL) measurements of single Zn_3P_2 NWs were performed with a microzone confocal Raman spectroscope (HORIBA Jobin Yvon, LabRam HR 800) equipped with a colour charge-coupled device (CCD). The 325 nm line of a He–Cd laser (Kimmon IK3301R-G) was used as the excitation source.

Zn_3P_2 SNW-MISFETs were fabricated as follows. First, the Zn_3P_2 NWs suspension was dropped on oxidized p-Si substrates (the SiO_2 layer is about 600 nm thick). Then, UV lithography, thermal evaporation and lift-off processes were used to fabricate the source and drain ohmic contact Ni/Au (10 nm/85 nm) electrodes. The underlying p-Si substrate was used as the back gate. The electrical transport measurements on the Zn_3P_2 SNW-MISFETs were conducted with a semiconductor parameters characterization system (Keithley 4200). During the measurement, the sources were grounded.

Results and discussion

A typical FESEM image of the as-synthesized Zn_3P_2 NWs is shown in Fig. 1a. The inset is a magnified FESEM image. We can see that each Zn_3P_2 NW has a smooth surface and uniform diameter along the growth direction. The average diameter of the NWs is about 100 nm, and the lengths are some tens of microns.

---

[a] *Department of Physics and State Key Lab for Mesoscopic Physics, Peking University, Beijing, 100871, People's Republic of China. E-mail: qingg@pku.edu.cn; lundai@pku.edu.cn*
[b] *Electron Microscopy Laboratory, Peking University, Beijing, 100871, People's Republic of China*

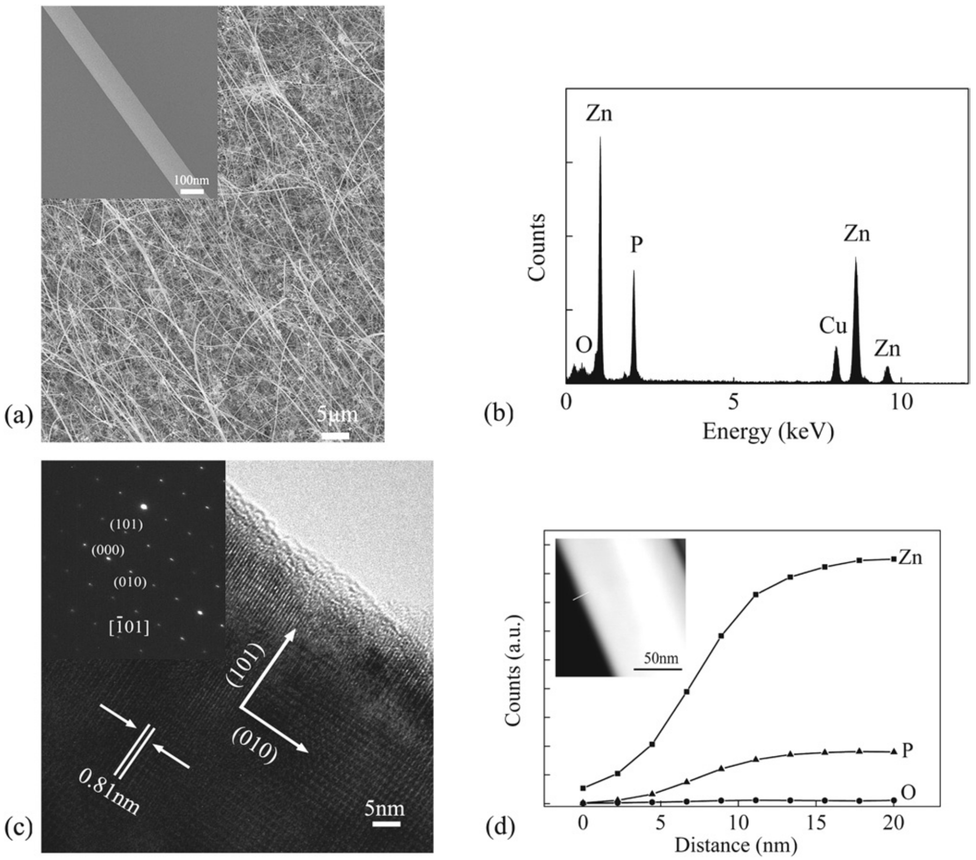

Fig. 1 (a) FESEM image of as-synthesized Zn_3P_2 NWs. The inset is a magnified image which shows the diameters of the NWs are about 100 nm. (b) EDX spectrum of an as-synthesized Zn_3P_2 NW. (c) HRTEM image of the nanowire. The inset shows the corresponding SAED pattern. (d) Line-scanning elemental mappings of Zn, P, and O along the route indicated by the white line in the inset. The inset is the HAADF-STEM image of the NW.

Fig. 1b shows the EDX spectrum taken from one such NW. It consists mainly of Zn and P signals with an atomic ratio of ~3 : 2, and a small amount of O. The signal of Cu is from the copper grid used for TEM observation.

Fig. 1c shows a HRTEM image of the single Zn_3P_2 NW. Crystal planes with the spacing distances of about 0.81 nm and 0.66 nm can be seen along and perpendicular to the growth direction, respectively. According to JCPDS (JCPDS card no 65-2854) data, the corresponding planes can be indexed as the tetragonal Zn_3P_2 (010) and (101) planes, respectively. The inset of Fig. 1c is the corresponding selected area electron diffraction (SAED) pattern recorded along the [$\bar{1}$01] zone axis. The HRTEM image together with the SAED pattern reveals that the Zn_3P_2 NW is a single crystal with the tetragonal structure, and its growth direction is [010]. In addition, we can see a thin amorphous layer on the surface of the Zn_3P_2 NW. The EDX spectrum taken from the amorphous layer shows that it consists mainly of Zn and P signals with an atomic ratio of ~3 : 2. In order to further investigate the spatial distribution of the atomic contents across the NW, line-scanning elemental mappings of Zn, P, and O were also conducted as shown in Fig. 1d. The inset is the HAADF-STEM image of the NW, and the line-scanning was performed on the white line. The small amount of O is distributed almost uniformly along the radial direction, which may result from the unavoidable oxygen adsorption during the TEM sample preparation processing. Therefore, we think the thin amorphous surface layer may result from degradation of Zn_3P_2 NW on exposure to the electron beam.

Fig. 2 shows the photoluminescence (PL) spectrum for a single Zn_3P_2 NW. We can see a strong emission centered around 770 nm, which may result from exciton emission near the band edge.[16]

Fig. 3a shows the source–drain current (I_{DS}) *versus* source–drain voltage (V_{DS}) curves at various gate biases (V_G) of a typical Zn_3P_2 SNW-MISFET. The inset is the schematic illustration of the Zn_3P_2 SNW-MISFET. For identical V_{DS}, the I_{DS} decreases when V_G varies from −1 V to +7 V. This characteristic shows the Zn_3P_2 NW is of p-type. From the I_{DS}–V_{DS} curve measured at $V_G = 0$, the resistivity (ρ) is calculated to be about 1.96 Ω cm.

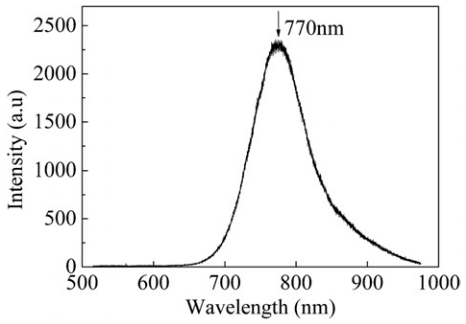

Fig. 2 The PL spectrum of a single Zn_3P_2 NW.

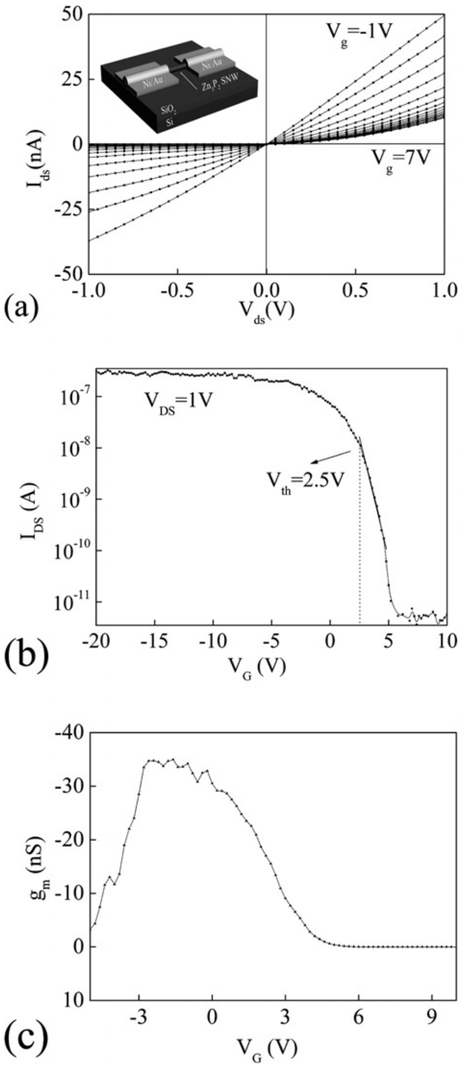

Fig. 3 (a) I_{DS}–V_{DS} characteristics of Zn_3P_2 SNW-MISFET measured at room temperature (RT) under gate bias ranging from −1 V to +7 V with a step of 0.5 V. The inset is a schematic illustration of the device. (b) The log I_{DS}–V_G curve of the SNW-MISFET at V_{DS} = 1 V. (c) The g_m–V_G curve of the MISFET at V_{DS} = 1 V.

Fig. 3b shows the I_{DS}–V_G curve on an exponential scale measured at V_{DS} = 1 V. The on–off ratio is obtained to be about 4×10^4. From the linear region of the curve, the threshold gate voltage (V_{th}) can be obtained to be about 2.5 V. The absolute value of the maximum transconductance ($g_m = dI_{DS}/dV_G$) estimated is about 35 nS, as shown in Fig. 3c. The channel mobility of the device μ_h can be estimated to be about 42.5 cm^2 V^{-1} s^{-1} (which is even higher than those of bulk Zn_3P_2 single crystal materials (~20 cm^2 V^{-1} s^{-1})[25]) with the equation $\mu_h = |g_m|\{L^2/[C(V_G - V_{th})]\}$.[26] Here, L is the channel length (40 μm) of the SNW-MISFET, the capacitance $C = 2\pi\varepsilon\varepsilon_0 L/[\ln(2h/r)]$,[26] where ε is the relative dielectric constant of SiO_2 (= 3.9), h (600 nm) is the thickness of the silicon oxide layer, and r (50 nm) is the nanowire radius. The hole concentration (p) can be estimated to be about 5.6×10^{16} cm^{-3} from the equation $p = CV_{th}/(e\pi r^2 L)$.[26] We can also obtain the p value from the equation $p = 1/\rho e\mu_h$ to be about 7.1×10^{16} cm^{-3}, which is close to the above value.

Conclusion

In conclusion, we report a CVD method to synthesise high quality Zn_3P_2 NWs, and we also fabricate p-type Zn_3P_2 SNW-MISFETs for the first time. Electrical measurement results of a typical p-type Zn_3P_2 SNW-MISFET indicate that the hole mobility and hole concentration of the Zn_3P_2 NWs are about 42.5 cm^2 V^{-1} s^{-1} and 5.6×10^{16} cm^{-3}, respectively. The obtained hole mobility of the Zn_3P_2 NW is so far the highest reported value for Zn_3P_2 materials (including the bulk Zn_3P_2 single crystal[25]). The on–off ratio of the typical p-type SNW-MISFET is about 4×10^4, and its threshold gate voltage and maximum transconductance are 2.5 V and 35 nS, respectively.

Acknowledgements

This work was supported by the National Natural Science Foundation of China under grant nos. 60576037, 10774007, 10574008, 50732001, and National Basic Research Program of China (Nos. 2006CB921607, 2007CB613402).

References

1 X. Duan, Y. Huang, R. Agarwal and C. M. Lieber, *Nature*, 2003, **421**, 241.
2 T. Gao, Q. H. Li and T. H. Wang, *Appl. Phys. Lett.*, 2005, **86**, 173105.
3 A. Pan, D. Liu, R. Liu, F. Wang, X. Zhu and B. Zou, *Small*, 2005, **1**, 980.
4 J. S. Jie, W. J. Zhang, Y. Jiang, X. M. Meng, Y. Q. Li and S. T. Lee, *Nano Lett.*, 2006, **6**, 1887.
5 P. Andrea, C. Elisabetta, S. Giorgio, J. Zhou, S. Z. Deng, N. S. Xu, Y. Ding and Z. L. Wang, *Appl. Phys. Lett.*, 2006, **88**, 203101.
6 R. M. Ma, L. Dai, H. B. Huo, W. Q. Yang, G. G. Qin, P. H. Tan, C. H. Huang and J. Zhen, *Appl. Phys. Lett.*, 2006, **89**, 203120.
7 Y. Cui and C. M. Lieber, *Science*, 2001, **291**, 851.
8 J.-H. Ahn, H.-S. Kim, K. J. Lee, S. Jeon, S. J. Kang, Y. Sun, R. G. Nuzzo and J. A. Rogers, *Science*, 2006, **314**, 1754.
9 A. Javey, S. Nam, R. S. Friedman, H. Yan and C. M. Lieber, *Nano Lett.*, 2007, **7**, 773.
10 G. Yu, A. Cao and C. M. Lieber, *Nat. Nanotechnol.*, 2007, **2**, 372.
11 J. Goldberger, A. I. Hochbaum, R. Fan and P. Yang, *Nano Lett.*, 2006, **6**, 973.
12 R. M. Ma, L. Dai and G. G. Qin, *Nano Lett.*, 2007, **7**, 868.
13 M. C. McAlpine, R. S. Friedman, S. Jin, K.-H. Lin, W. U. Wang and C. M. Lieber, *Nano Lett.*, 2003, **3**, 1531.
14 R. S. Friedman, M. C. McAlpine, D. S. Ricketts, D. Ham and C. M. Lieber, *Nature*, 2005, **434**, 1085.
15 R. M. Ma, L. Dai, H. B. Huo, W. J. Xu and G. G. Qin, *Nano Lett.*, 2007, **7**, 3300.
16 R. S. Yang, Y. L. Chueh, J. R. Morber, R. Snyder, L. J. Chou and Z. L. Wang, *Nano Lett.*, 2007, **7**, 269.
17 K. Kakishita, K. Aihara and T. Suda, *Appl. Surf. Sci.*, 1994, **80**, 281.
18 J. Misiewicz, L. Bryja, K. Jezierski, J. Szatkowski, N. Mirowska, Z. Gumienny and E. Placzekpopko, *Microelectron. J.*, 1994, **25**, R23.
19 R. Sathyamoorthy, C. Sharmila, P. Sudhagar, S. Chandramohan and S. Velumani, *Mater. Charact.*, 2007, **58**, 730.
20 H. F. Bao, X. Q. Cui, C. M. Li, Y. Gan, Jun Zhang and Jun Guo, *J. Phys. Chem. C*, 2007, **111**, 12279.
21 G. Z. Shen, C. H. Ye and D. Golberg, *Appl. Phys. Lett.*, 2007, **90**, 073115.
22 G. Z. Shen, Y. Bando and D. Golberg, *J. Phys. Chem. C*, 2007, **111**, 5044.
23 G. Z. Shen, Y. Bando, C. H. Ye, X. L. Yuan, T. Sekiguchi and D. Golberg, *Angew. Chem., Int. Ed.*, 2006, **45**, 7568.
24 G. Z. Shen, Y. Bando, J. Q. Hu and D. Golberg, *Appl. Phys. Lett.*, 2007, **88**, 143105.
25 N. Mirowska and J. Misiewicz, *Mater. Sci. Eng., B*, 2006, **130**, 49.
26 Y. Huang, X. F. Duan, Y. Cui and C. M. Lieber, *Nano Lett.*, 2003, **3**, 343.